Divertor electron temperature and impurity diffusion measurements with a spectrally resolved imaging radiometer[a)]

D. J. Clayton,[1,b)] M. A. Jaworski,[2] D. Kumar,[1] D. Stutman,[1] M. Finkenthal,[1] and K. Tritz[1]
[1]*Johns Hopkins University, Baltimore, Maryland 21218, USA*
[2]*Princeton Plasma Physics Laboratory, Princeton, New Jersey 08543, USA*

(Presented 8 May 2012; received 4 May 2012; accepted 8 June 2012;
published online 23 July 2012)

A divertor imaging radiometer (DIR) diagnostic is being studied to measure spatially and spectrally resolved radiated power $P_{rad}(\lambda)$ in the tokamak divertor. A dual transmission grating design, with extreme ultraviolet (~20–200 Å) and vacuum ultraviolet (~200–2000 Å) gratings placed side-by-side, can produce coarse spectral resolution over a broad wavelength range covering emission from impurities over a wide temperature range. The DIR can thus be used to evaluate the separate P_{rad} contributions from different ion species and charge states. Additionally, synthetic spectra from divertor simulations can be fit to $P_{rad}(\lambda)$ measurements, providing a powerful code validation tool that can also be used to estimate electron divertor temperature and impurity transport. © *2012 American Institute of Physics*. [http://dx.doi.org/10.1063/1.4732066]

I. INTRODUCTION

As divertor heat loads increase with advancements in magnetic fusion devices, it has become important to better understand how power is radiated in the divertor and how this can be manipulated to reduce these heat loads. While bolometers are often implemented to measure total radiated power P_{rad}, and spectrometers are used to identify which ion species are present in the divertor, this is often insufficient to distinguish which species dominate P_{rad} in various regions of the divertor. For example, in NSTX, increasing the deposition of lithium onto the divertor floor has been shown to increase P_{rad} in the divertor and reduce the heat load on the plasma facing components (PFCs). It is currently unknown if this is due to the introduction of lithium ions into the divertor plasma or to increased carbon densities resulting from lithium-induced edge localized mode suppression. Lithium ions in coronal equilibrium are not sufficient to radiate significant power in the divertor, but large impurity transport could lead to a non-coronal lithium charge state distribution that is sufficient to contribute to the total P_{rad}.[1,2] A divertor imaging radiometer (DIR), a UV diagnostic with 1D spatial resolution and coarse wavelength resolution covering a wide spectrum, could be used to validate divertor simulations by measuring spatially resolved radiated power $P_{rad}(\lambda)$ while identifying the radiating species. Additionally, with accurate divertor simulations, a $P_{rad}(\lambda)$ measurement can provide an electron temperature measurement and cross-field impurity transport estimates in the divertor.

The proposed DIR is a low-cost, compact diagnostic that utilizes two transmission gratings, one in the vacuum ultraviolet (VUV) spectral range (~200–2000 Å with 50 Å resolution) and the other in the extreme ultraviolet (XUV) range (~20–200 Å with 10 Å resolution), to produce a radiated power measurement with coarse spectral resolution. The spectrally resolved 1D image is measured directly by an x-ray CCD, providing an angular resolution of about 0.33° and time resolution ≥10 ms, with ~0.5% error from readout noise and photon statistics for typical UV brightnesses. Ideally, the diagnostic would be installed on a divertor diagnostic port with lines of sight that do not pass through the main plasma volume. If such a port is unavailable, the DIR could alternately be installed on any port with a view of the divertor, though modeling may be required to subtract background emission from the main plasma volume. Two radiometers could provide a two-dimensional measurement of the radiated power in the divertor. The detailed design of the DIR, along with a description of measurements performed with this hardware on the bench, can be found in these proceedings.[3]

II. SPECTRALLY AND SPATIALLY RESOLVED RADIATED POWER MEASUREMENTS

To study the capabilities of a DIR diagnostic, the NSTX divertor was modeled with the OEDGE code.[4] Interpretive modeling of medium triangularity discharges was performed using divertor target data from the NSTX high-density Langmuir probe array. Temperature and density were determined using a kinetic probe interpretation[5] and were found to be consistent with infrared diagnosis of PFC heat flux as well as spectroscopic analyses of the discharges. In these discharges, the outboard divertor leg was attached to the target while the inboard divertor was detached. The outboard divertor leg was reconstructed using generalized, 2-point Runge-Kutta integration along each flux tube. The inboard detached plasma was modeled using heuristic methods first applied to C-Mod and DIII-D.[6] The Monte-Carlo hydrogenic code, EIRENE, was used to calculate the neutral solution consistent with the background plasma. Impurities were modeled using the Monte-Carlo impurity code DIVIMP.[7] Intrinsic impurities were

[a)]Contributed paper, published as part of the Proceedings of the 19th Topical Conference on High-Temperature Plasma Diagnostics, Monterey, California, May 2012.
[b)]Electronic mail: dclayton@pppl.gov.

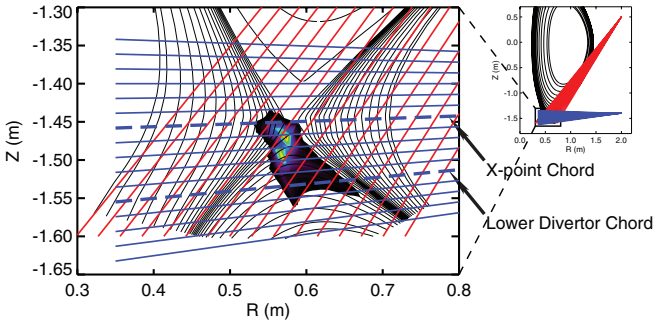

FIG. 1. Divertor flux surfaces, with lines representing detector chords from divertor and mid-plane ports. The highlighted X-point chord and lower divertor chord from the divertor port are used to produce subsequent figures. A contour plot of 123 Å emission from Ne VI is included as an example.

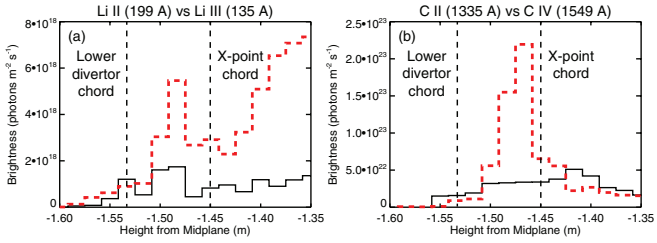

FIG. 3. (a) Spatial distribution of simulated Li III brightness (135 Å, red dashed line) versus Li II brightness (199 Å, solid black line), as measured by a DIR on a divertor port. (b) C IV brightness (1549 Å, red dashed line) versus C II brightness (1335 Å, solid black line). The height from mid-plane is defined as the height of a chord at the major radius of the X-point (R = 0.58 m).

generated by physical and chemical sputtering of the PFC surfaces (in the case of Li, only physical sputtering applies). Injected impurities were introduced by a simulated, thermal gas puff in the private flux region of the plasma. Cross-field impurity transport was varied as described below.

From the results of the OEDGE simulations, the impurity UV emissivity was calculated using the Atomic Data and Analysis Structure database.[8] Line emission from electron excitation, recombination, charge exchange with neutral deuterium (in the case of carbon), and continuum emission from free-free and free-bound interactions were all calculated, though electron excitation emission was the dominant source of radiated power throughout most of the divertor. The UV brightness that would be measured by a DIR is found by line-integrating the resulting emissivity. Figure 1 shows the flux surfaces used by OEDGE and the detector chords used for line integration.

The DIR directly measures P_{rad}, a result that is independent of any modeling and can thus be used to validate P_{rad} predictions from divertor models. Figures 2 and 3 show the results of OEDGE simulations of carbon and lithium. The

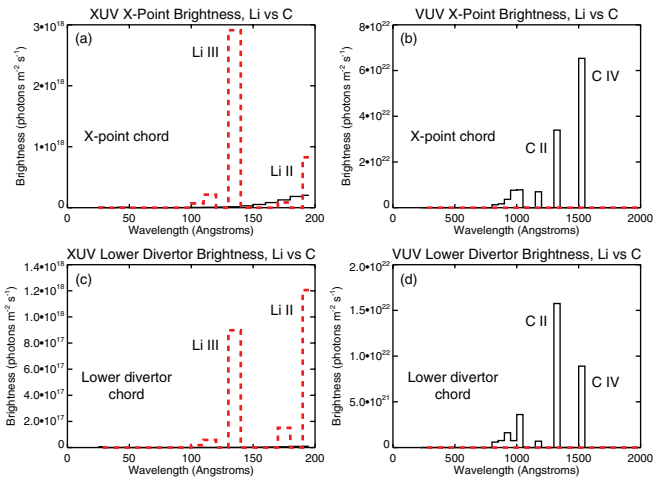

FIG. 2. (a) and (b) Simulated UV brightness from carbon (solid black lines) and lithium (dashed red lines) measured by the DIR chord through the X-point. (c) and (d) Brightness measured by the lower divertor chord labeled in Fig. 1.

relative sputtering yields of Li and C from lithium-coated carbon are unknown; for the purposes of these simulations, the total number of carbon and lithium ions in the divertor are set equal to one another. As shown in Fig. 2, C II and C IV are the primary radiators in the VUV range, with Li II and Li III dominating XUV emission, although this XUV emission is several orders of magnitude weaker than the carbon emission. C IV and Li III emission are peaked around the X-point, while the C II and Li II emission profiles appear flat, as most of this radiation comes from the cold plasma near the vessel wall. Figure 3 shows brightness profiles that would be measured by a radiometer installed on a divertor port. These results demonstrate that DIR measurements could be used to test these divertor models and determine which species are actually radiating in each region of the divertor.

III. DIVERTOR T_e AND $D_\perp$ MEASUREMENTS WITH IMPURITY SEEDING

Additional information can be obtained from DIR measurements with proper modeling of the divertor plasma. UV emissivity $\epsilon \approx n_e n_Z R(T_e)$, where R is a function dependent only on T_e (a very weak density dependence is ignored). Variations in n_e and n_Z thus only affect the total P_{rad} while leaving the spectral profile essentially unchanged, while variations in T_e impact spectral features such as line ratios. By comparing measured spectral features to the results of simulations, T_e can be inferred from DIR measurements. To maximize the accuracy of these T_e measurements, the divertor can be seeded with non-intrinsic impurities with emissivities that are sensitive to small temperature changes in the T_e range found in the divertor. Cross-field impurity transport, represented in the simulations with a diffusion coefficient $D_\perp$, can impact the charge state distribution of the impurity, spatially spreading out each charge state from a coronal equilibrium. The effects of T_e and $D_\perp$ on UV emission are distinct and can be demonstrated using an example of neon seeding in the NSTX divertor.

Neon in the NSTX divertor would emit strongly in both the XUV and VUV range, though the XUV emission exhibits more spectral features and less background emission from carbon. Ne VI line emission at 123 Å dominates the

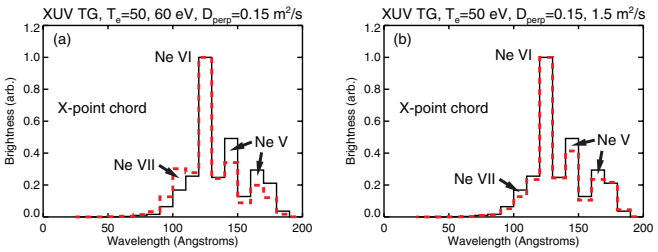

FIG. 4. (a) Simulated Ne brightness from a 50 eV plasma (black solid line) versus a 60 eV plasma (red solid line), both with $D_\perp = 0.15$ m^2/s. (b) Ne brightness from a plasma with $D_\perp = 0.15$ m^2/s (solid) versus $D_\perp = 1.5$ m^2/s (dashed), both with $T_e = 50$ eV. The temperatures refer to T_e at the X-point, and the normalized spectra are from the X-point chord.

XUV radiated power near the X-point in OEDGE simulations, though emission from Ne IV and Ne V plays a larger role in the colder regions of the divertor. The effects of a small increase in temperature on the measured spectra, in this case an increase of T_e at the X-point from 50 eV to 60 eV, can be seen in Fig. 4(a). When the spectra are normalized to the Ne VI emission, Ne VII emission increases while Ne V emission decreases, as expected. For comparison, the effects of cross-field impurity transport on the spectra are shown in Fig. 4(b). When the impurity diffusion coefficient $D_\perp$ is increased an order of magnitude, from 0.15 m^2/s to 1.5 m^2/s, the spectrum measured through the X-point remains relatively unchanged. To better see the effects of temperature versus transport on the measured UV brightness, spatial profiles of the Ne VI 123 Å emission are shown in Fig. 5. The view from the divertor port shows that increasing T_e shifts the Ne VI emission down towards the divertor floor as the plasma becomes hotter everywhere. When $D_\perp$ is increased, Ne VI begins to diffuse upwards into the hotter plasma region, flattening the spatial profile. Figures 5(c) and 5(d) show that the diffusive flattening of the profile can also be seen from a mid-plane port, though the effects of increased T_e are less obvious.

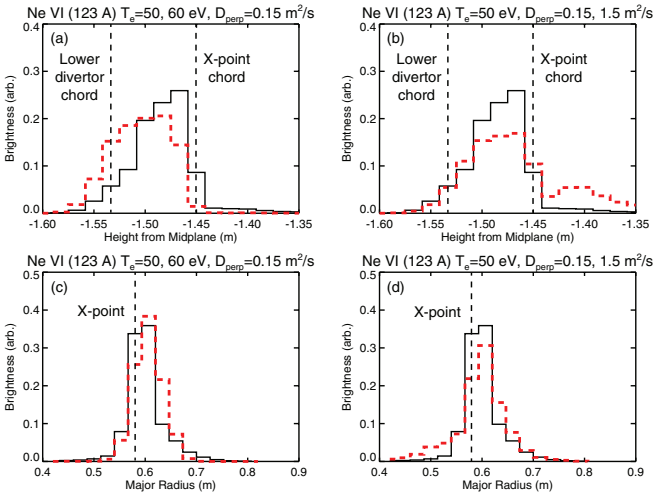

FIG. 5. (a) Vertical profile of simulated Ne VI brightness (123 Å) for $T_e = 50$ eV and 60 eV, with $D_\perp = 0.15$ m^2/s. (b) Ne VI brightness for $D_\perp = 0.15$ m^2/s and 1.5 m^2/s, with $T_e = 50$ eV. (c) and (d) Same scenario as in (a) and (b), but as viewed by a DIR on a mid-plane port. Major radius of a chord is defined at the height of the X-point ($Z = -1.45$ m).

To obtain estimates of T_e and $D_\perp$ from DIR measurements, minimization techniques can be used to vary T_e and $D_\perp$ in the divertor simulations to find the values that provide the best match to these measurements. Note that on experiments with additional divertor temperature and density diagnostics, a DIR could then be used to further validate divertor simulations.

IV. SUMMARY

In summary, a transmission-grating based radiometer is an inexpensive, compact solution for diagnosing radiated power in a tokamak divertor, and can be used to identify the radiating species. This DIR can be an essential tool in validating simulations of a plasma region that is not yet well understood. Additionally, this diagnostic can be used in conjunction with proper divertor modeling to provide an estimate of the electron temperature profile and the value of the impurity cross-field diffusion. The addition of a second such diagnostic would provide a 2D profile of $P_{rad}(\lambda)$ and T_e.

ACKNOWLEDGMENTS

This work was supported by (U.S.) Department of Energy (DOE) Contract Nos. DE-AC02-09CH11466 and DE-FGO2-86ER53214.

[1]T. D. Rognlien and M. E. Rensink, Phys. Plasmas **9**, 2120 (2002).
[2]S. Mirnov, J. Nucl. Mater. **390–391**, 876 (2009).
[3]D. Kumar, D. J. Clayton, M. Parman, D. Stutman, K. Tritz, and M. Finkenthal, Rev. Sci. Instrum. **83**, 10E511 (2012).
[4]P. C. Strangeby, J. D. Elder, J. A. Boedo, B. Bray, N. H. Brooks, M. E. Fenstermacher, M. Groth, R. C. Isler, L. L. Lao, S. Lisgo, G. D. Porter, D. Reiter, D. L. Rudakov, J. G. Watkins, W. P. West, and D. G. Whyte, J. Nucl. Mater. **313–316**, 883 (2003).
[5]M. A. Jaworski, M. G. Bell, T. K. Gray, R. Kaita, J. Kallman, H. Kugel, B. LeBlanc, A. McLean, S. A. Sabbagh, V. A. Soukhanovskii, D. P. Stotler, and V. Surla, "Modification of the electron energy distribution function during lithium experiments on the National Spherical Torus Experiment," Fusion Eng. Des. (in press).
[6]S. Lisgo, P. C. Strangeby, J. D. Elder, J. A. Boedo, B. D. Bray, N. H. Brooks, M. E. Fenstermacher, M. Groth, D. Reiter, D. L. Rudakov, J. G. Watkins, W. P. West, and D. G. Whyte, J. Nucl. Mater. **337–339**, 256 (2005).
[7]J. D. Elder, P. C. Strangeby, D. G. Whyte, S. L. Allen, A. McLean, J. A. Boedo, B. D. Bray, N. H. Brooks, M. E. Fenstermacher, M. Groth, C. J. Lasnier, S. Lisgo, D. L. Rudakov, W. R. Wampler, J. G. Watkins, and W. P. West, J. Nucl. Mater. **337–339**, 79 (2005).
[8]H. P. Summers, "Atomic Data and Analysis Structure," Tech. Rep. JET-IR(94)06 (JET Joint Undertaking, Oxfordshire: Abingdon, 1994).